NANO LETTERS

2007
Vol. 7, No. 11
3372−3376

Efficiency Enhancements in Solid-State Hybrid Solar Cells via Reduced Charge Recombination and Increased Light Capture

Henry J. Snaith,*,†,‡ Adam J. Moule,§,|| Cédric Klein,† Klaus Meerholz,§ Richard H. Friend,‡ and Michael Grätzel†

Institut de Chimie Physique, École Polytechnique Fédérale de Lausanne, CH-1015 Lausanne, Switzerland, Cavendish Laboratory, Madingley Road, Cambridge CB3 0HE, United Kingdom, and Institut für Physikalische Chemie, Luxemburstrasse 116, 50939 Köln, Germany

Received July 9, 2007; Revised Manuscript Received September 21, 2007

ABSTRACT

We compare a series of molecular sensitizers in dye-sensitized solar cells containing the organic hole transporter 2,2′,7,7′-tetrakis(*N*,*N*-di-*p*-methoxypheny-amine)-9,9′-spirobifluorene (spiro-MeOTAD). Charge recombination is reduced by the presence of "ion-coordinating" moieties on the dye, with the longest electron lifetime and highest solar cell efficiency achieved using a novel sensitizer with diblock alkoxy-alkane pendent groups. By further increasing the optical path length in the active layer, we achieve a power conversion efficiency of over 5% under simulated sun light.

Dye-sensitized solar cells (DSCs) promise to offer a solution to low-cost large-area photovoltaic applications. They are fabricated from cheap, easily processable materials, deriving their competitive performance from judicious molecular design and control of nanoarchitecture rather than particularly impressive electronic characteristics of the individual materials. The standard structure of the dye-sensitized solar cell comprises an electrochemical cell composed of mesoporous titania sensitized with light-absorbing dye molecules and filled with a redox-active liquid electrolyte (iodide/triodide based).[1] Under light absorption, photogenerated electrons are injected from the dye into the conduction band of the TiO_2, which are subsequently transported to and collected at the anode. There has been much work developing new light-sensitizer molecules and engineering of the titania/dye/electrolyte interface in order to enhance the charge generation and separation process in the composite.[2−7] The function of the electrolyte is to "regenerate" the oxidized dye and to transport the "holes" to the external circuit. Because of concerns over solvent leakage and corrosion, recent attention has been focused on replacing this electrolyte with solid-state hole transporter alternatives to create fully electronic DSCs.[8−10] Significant advances have been made, although approaching the efficiency of the original electrochemical cell (ca. 10%) has proven to be illusive. One approach introduced relatively recently to replace the liquid electrolyte uses an organic hole transport material to create a hybrid (organic/inorganic) fully electronic DSC.[8] For this approach, spiro-MeOTAD has proven to be most successful due to its respectable charge carrier mobility,[11] amorphous nature, and high solubility. The latter two enabling material infiltration into mesoporous titania films of up to a few micrometers thickness. One of the main hurdles to achieving commercially viable power conversion efficiencies with cells incorporating spiro-MeOTAD is enhancing the light capture in the device. Presently for our system, the optimized device thickness is only 2 μm, resulting in the majority of the incident light over the absorbing region of the composite not being absorbed in the active medium (the absorption depth at 600 nm is around 10 μm). The optimized thickness is a compromise between light absorption and charge collection. The two issues that appear to be in need of addressing in order to improve charge collection are to enhance the electron diffusion length (L_D), which has been reported to be only a few micrometers in this composite,[12] and to improve the infiltration of spiro-MeOTAD into mesoporous titania.[13] An approach that should enhance the electron diffusion length

* Corresponding author. E-mail: h.snaith1@physics.ox.ac.uk.
† Institut de Chimie Physique, École Polytechnique Fédérale de Lausanne.
‡ Cavendish Laboratory.
§ Institut für Physikalische Chemie.
|| Current address: Department of Materials Science, UC Davis, Davis, CA 95616.

10.1021/nl071656u CCC: $37.00 © 2007 American Chemical Society
Published on Web 10/05/2007

is to increase the electron−hole recombination lifetime (τ_e) because $L_D = \sqrt{D_e \tau_e}$, where D_e is the effective electron diffusion coefficient. A third issue that could obviate the requirement for thicker films is to consider and improve the photonic structure of the cell such that close to complete light capture can occur in thin films (~2 μm). Here, we address the issues of increasing the electron diffusion length and improving the photonic structure of the solar cell. We investigate a series of ruthenium-based bipyridyl complex dye molecules that increase the electron lifetime in the composite. The longest electron lifetime and highest reported solar cell performance is demonstrated for a new sensitizer with diblock alkoxy-alkane pendent groups. Surprisingly, the optimized film thickness still remains around 2 μm, suggesting that electron−hole recombination is not the limiting loss in these devices. By further enhancing the optical path length in the solar cell, via altering the reflectivity of the counter electrode, we increase the collected current density and power conversion efficiency to over 5%, measured under simulated AM 1.5 solar illumination at an intensity of 126 mW cm^{-2}.

The solid-state dye-sensitized solar cells were fabricated and characterized as previously described,[8,14] albeit no chemical oxidant was added to spiro-MeOTAD.[15] The spectral mismatch of the solar simulator to the AM 1.5 solar spectrum was estimated over the entire photoactive wavelength range of the solar cells and the calibration diode following the method of Seaman.[16] The mismatch is calculated to be less than 2% between 400 and 750 nm, the active range of the solar cells. The solar cells were typically 0.16 cm^2, defined by the overlap of the FTO anode and metal cathode. Optical masks were occasionally employed to define the active area but made no noticeable difference to the measured photocurrent density. Transient open-circuit voltage decay measurements were performed by a method similar to that of O'Regan et al.:[17,18] A white light bias was generated from an array of diodes (Lumiled model LXHL-NWE8 whitestar) with red light pulsed diodes (LXHL-ND98 redstar, 0.2 s square pulse width, 100 ns rise and fall time) as the perturbation source, controlled by a fast solid-state switch. The voltage dynamics were recorded on a PC-interfaced Keithley 2400 sourcemeter with a 500 μs sampling time and a 5 μs response time to an abrupt change in load. The perturbation light source was set to a suitably low level such that the voltage decay kinetics were monoexponential. This enabled the charge recombination rate constants to be obtained directly from the exponential decay rate of the voltage decay.

It has been observed that the addition of bis(trifluoromethyl-sulfonyl)amine lithium salt (Li−TFSI) to spiro-MeOTAD successfully retards the recombination between electrons in the TiO_2 with holes in the spiro-MeOTAD, resulting in dramatic enhancements in solar cell performance.[19] We believe that the suppression of recombination is due to a Coulombic screening of the electrons in the TiO_2 and holes in the spiro-MeOTAD by lithium ions adsorbed to the titania surface. As well as being influenced by the ionic nature of the hole transporter matrix, it is apparent that the charge recombination can be influenced by the spatial extent of the dye molecules.[21] This illustrates that the dye can act as a potential barrier, increasing the distance over which the electron−hole recombination reaction occurs.[20] Which of these two processes is dominant in the complete solar cell is uncertain (Coulombic screening or potential barrier). Recently, we demonstrated that coordination of lithium ions, directly to the dye molecules, can further suppress charge recombination,[21,22] presumably due to an increased concentration of lithium ions near the TiO_2/dye/spiro-MeOTAD heterojunction. Here, we have synthesized a further series of "ion-coordinating" bipyridyl ruthenium complexes, the chemical structures of which are shown in Figure 1a. They have identical π conjugated units with differing pendent side chains of MeO (termed K63), tetra(ethylene glycol) (termed K51)[21,22] and tetra(ethylene glycol)-heptyl diblocks (termed K68), the synthesis procedures will be published elsewhere.[23] The light absorption in thin films of mesoporous TiO_2 sensitized with all three complexes is almost identical, as measured by UV−vis transmission spectroscopy. Solid-state dye-sensitized solar cells, fabricated using these dyes, show systematic improvements in short-circuit current, fill factor, and open-circuit voltage when the size of the pendent group is increased from MeO to tetra(ethylene glycol) and to tetra(ethylene glycol)-heptyl diblocks. Solar cells incorporating the K68 sensitizer (TEG-heptyl) outperform those incorporating all previously sensitizers exhibiting the highest reported efficiency for this type of DSC of 4.2% under AM 1.5 simulated sun light at 100 mW cm^{-2} illumination intensity (here using Au cathodes).

To understand why we observe this trend in device performance, we have performed small perturbation transient open-circuit voltage decay measurements on complete solar cells: A bias white light source is used to generate charge in the cell. When the bias light intensity is increased, more light is absorbed in the dye and hence more electrons are injected into the TiO_2, filling sub-band gap electronic states in the TiO_2. If no charge is being collected, the voltage generated in the solar cell is considered to be the difference in energy between the quasi-Fermi level for electrons (E_{Fn}) in the TiO_2 and the quasi-Fermi level for holes (E_{Fp}) in the spiro-MeOTAD. A low-intensity red light pulsed diode is used to perturb the system, resulting in extra electrons being injected from the dye into states just above E_{Fn} in energy in the TiO_2. The distribution of states in the TiO_2 is represented schematically in Figure 1c. In reality, there is also an energetic spread of states in spiro-MeOTAD and all the arguments concerning sub-band gap states in TiO_2 should also apply. However, to simplify argumentation, we shall only discuss electronic states in TiO_2. The transient voltage perturbation is recorded on an oscilloscope or sourcemeter. If the perturbation light source is set to a suitably low level, the voltage decay kinetics are monoexponential and the decay rate of the voltage perturbation, measured at open-circuit, corresponds directly to the recombination rate constant of the charges in the solar cell. In Figure 1d, we present the estimated charge recombination rate constant (k_{rec}) versus intensity of the white light bias source. We observe that the

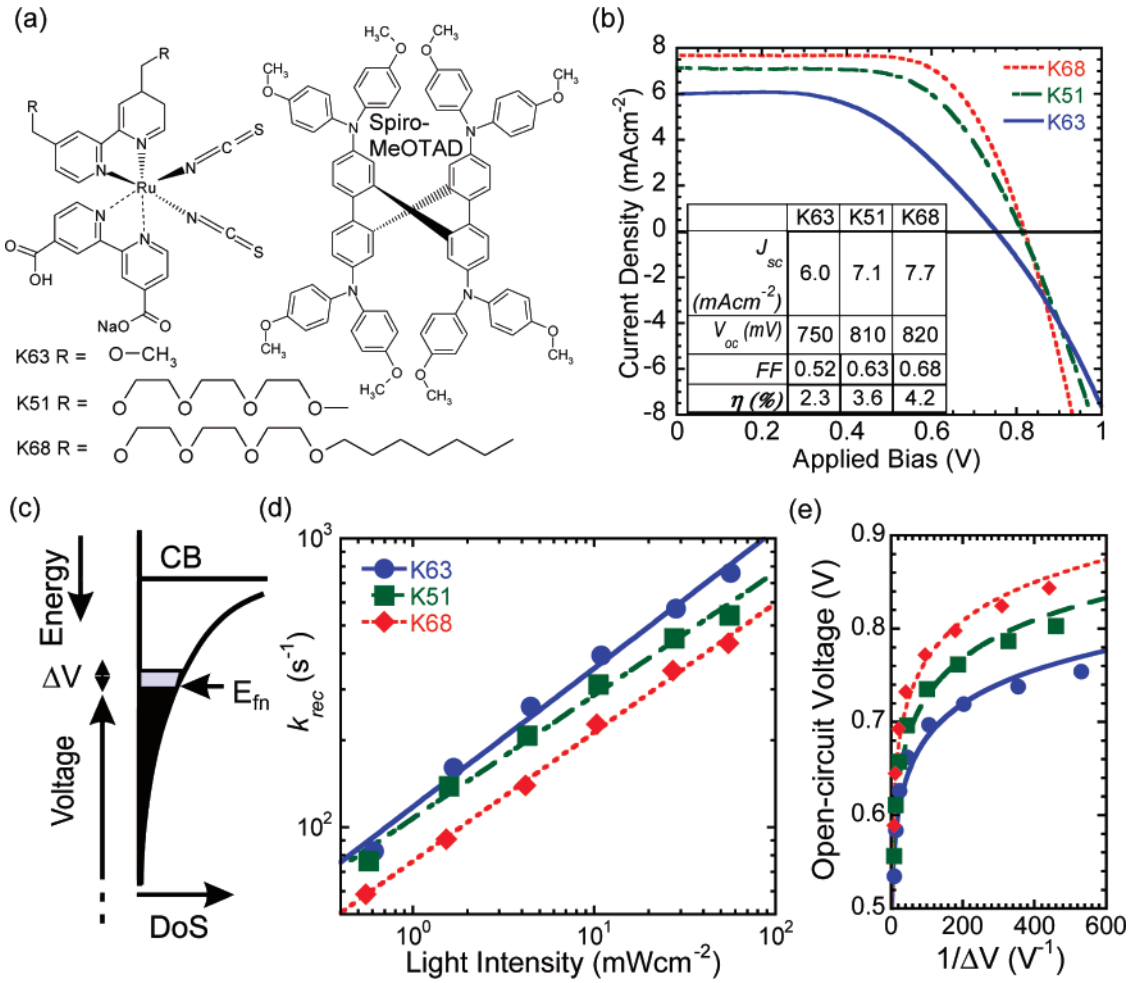

Figure 1. (a) Chemical structure of the Ru-bipyridyl sensitizers synthesized and employed in this study and that of the hole transporter spiro-MeOTAD. (b) Current−voltage (*JV*) curves for solid-state DSCs incorporating the three sensitizers, measured under simulated AM 1.5 solar illumination at an intensity of 100 mW cm^{-2}. Inset: Solar cell performance parameters calculated from the *JV* curves. (c) Illustration of the density-of-states (DoS) distribution in the mesoporous TiO_2 films. The dark region below the E_{Fn} represents states with a probability greater than $^1/_2$ of being filled. ΔV represents the change in the E_{Fn} induced by the perturbation light source. (d) Charge recombination rate constant (k_{rec}), estimated from small perturbation open-circuit voltage decay measurements vs bias white light intensity for solid-state DSCs incorporating the three sensitizers (see legend). (c) Open-circuit voltage vs the reciprocal of the voltage perturbation extracted from the measurements in (d). This gives an estimation of the relative position of the energy levels in the TiO_2 with respect to those in the spiro-MeOTAD.

k_{rec} reduces at all light intensities as we go from K63 to K51 to K68. This could explain the increased current collection observed in the devices if charge collection at short-circuit is hampered by bimolecular recombination, however, as we discuss below, we note that this may not be the case. The reduced recombination could also explain the increased open-circuit voltage. To further investigate this, we can probe the density-of-states in the composite more closely, giving information concerning the relative position of the TiO_2 and the spiro-MeOTAD energy levels: For these measurements, the differential capacitance of the film (C) can be estimated using $C = \Delta Q/\Delta V_0$, where ΔV_0 is the initial voltage perturbation induced by the light pulse and ΔQ is the extra injected charge, which induces this voltage perturbation. Because the perturbation light intensity is kept constant for all measurements, to a first-order approximation, ΔQ can be considered a constant for all measurements and therefore the capacitance is proportional to $1/\Delta V$. As stated earlier, the open-circuit voltage is considered to be the difference between the quasi-Fermi level for electrons in the TiO_2 and holes in the spiro-MeOTAD ($E_{Fn} - E_{Fp}$). Therefore, plotting the open-circuit voltage versus $1/\Delta V$ gives information concerning the relative position of the electronic sites in the TiO_2 with respect to the reference potential, here E_{Fp}. Assuming the same density-of-states distribution for all three systems, this plot gives information concerning the relative position of the energy levels in TiO_2 with respect to those in spiro-MeOTAD, i.e., if there are any changes to the induced dipole moment at the heterojunction. This is plotted for the cells containing the three dyes in Figure 1e. The lines are logarithmic fits to the data, consistent with an exponential tail to the density-of-states in TiO_2. Most notably, the points are fitted with similar logarithmic curves but with different offsets. This implies that the difference in energy between the TiO_2 and the spiro-MeOTAD energy levels has increased going from K63 to K51 to K68. This finding is consistent with the oxyethylene side chains coordinating lithium ions,[21,22] with the increased positive charge density inducing

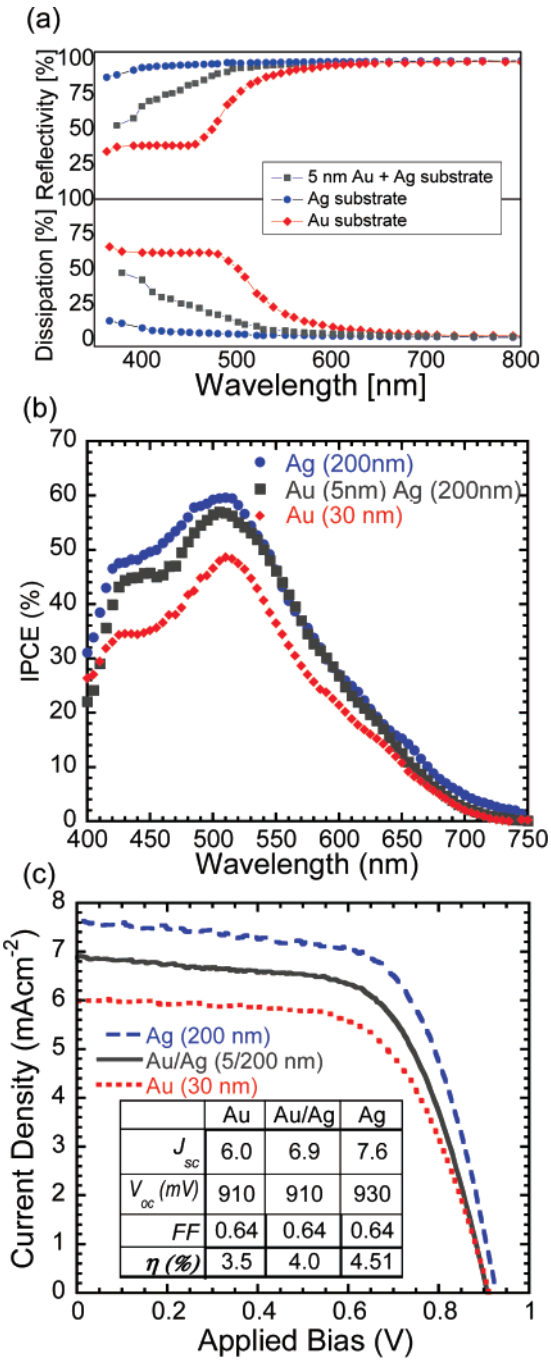

	Au	Au/Ag	Ag
J_{sc}	6.0	6.9	7.6
V_{oc} (mV)	910	910	930
FF	0.64	0.64	0.64
η (%)	3.5	4.0	4.51

Figure 2. (a) Dissipation and reflectivity from Au (30 nm) (red diamonds), Ag (200 nm) (blue circles), and a bilayer of Au and Ag (5/200 nm) (black squares) surfaces, calculated from ellipseometric measurements from the metals evaporated on glass slides. (b) Spectral response of solid-state DSCs incorporating K68 sensitizer with Au (30 nm), Ag (200 nm), and bilayer Au/Ag (5/200 nm) cathodes. (c) Current voltage curves for similar devices to those in Figure 2b measured under simulated AM 1.5 solar illumination at an intensity of 100 mW cm^{-2}. Table inset: Solar cell performance parameters calculated from these *JV* curves.

a dipole offset in this favorable direction. We also note that we cannot rule out the possibility that the oxyethylene moieties may themselves contact the TiO_2 and passivate surface defect sites (Ti_3^+), which could also contribute to the shift in surface potential.

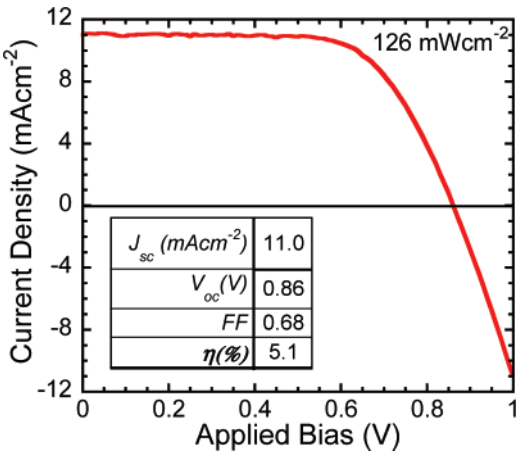

J_{sc} (mAcm^{-2})	11.0
V_{oc}(V)	0.86
FF	0.68
η(%)	5.1

Figure 3. Current−voltage curve for our best performing solar cell incorporating pure Ag electrodes and K68 molecular sensitizer, measured under simulated AM 1.5 solar illumination at an intensity of 126 mW cm^{-2}.

We have demonstrated that by controlling the charge recombination significant improvements in device performance can be achieved. Surprisingly, even though we have approximately halved the recombination rate constant, comparing K63 to K68, we still find that the optimized solar cell thickness is around 2 μm. This suggests that the main limitation to device thickness is not the limited electron diffusion length but another factor such as incomplete filling of the mesoporous TiO_2 with spiro-MeOTAD.[13] Because of this ever-present limitation of device thickness, the charge collection efficiency from incident sun light still remains relatively low. We also note that if the electron−hole recombination is not limiting the current collection, then the enhanced short-circuit current when comparing this series of dyes is rather perplexing. It suggests that charge generation efficiency from absorbed photons under working conditions may be significantly influenced by the pendent groups on the dye molecules. This may be due to subtle changes to the dye orientation and energy level arrangement at the interface. Alternatively, spiro-MeOTAD infiltration into the mesoporous TiO_2 may be influenced by the chemical nature of the pendent groups on the ruthenium complexes. Both of these processes are difficult to quantify although should be investigated in further work.

Here, we consider a route to increase the optical path length in the device. Au is typically used as the hole-collecting cathode due to its large work function. However, Au is poorly reflective in the visible region of the spectrum, dissipating the majority of the incident light. In Figure 2a, we show the calculated percentage of incident light that is either dissipated in the metal or reflected from the metal surface for an optically thick Au film, an optically thick Ag film, and a bilayer of a 5 nm thick Au film on a Ag substrate. The optical constants for the metal surfaces were measured using spectroscopic ellipsometry (Nanofilm with EP3 software) and are displayed for an air/metal interface for normal incidence. The reflectivity of the three metal electrodes at the maximum in spectral response (~510 nm) for these devices is decisively different. The reflectivity from Au is only 56% as compared to 96% for Ag and 89% for Au/Ag

(5/200 nm). The reflectivity of the Au substrate decreases still further to 25% by 400 nm. By increasing the reflectivity of the back electrode, less light is dissipated into the metal and more can be captured by increasing the optical path length of the active material. In Figure 2b, we show the spectral response of solid-state DSCs incorporating K68 sensitizer with Au (30 nm) Au/Ag (5/200 nm) and pure Ag (200 nm) electrodes. As predicted from the reflectivity calculations, the photocurrent is systematically enhanced by incorporating the more reflective electrodes, especially in the blue regions of the spectrum where the reflectivity from Au is low. When measured under simulated sun light, we also observe comparable enhancements in photocurrent, with negligible change to both fill factor and open-circuit voltage, Figure 2c. It is at first surprising that the open-circuit voltage does not drop when the spiro-MeOTAD is directly contacted by Ag because the work function of Ag is nominally 4.4 eV, which should result in a negative built-in potential (the transparent cathode, SnO_2:F, is nominally 4.8 eV). This suggests that Fermi-level pinning may occur at the spiro-MeOTAD/metal contact, resulting in good electrical contact and no loss in voltage. This is consistent with recent photoelectron spectroscopy studies on organic-metal interfaces.[24] Alternatively, a thin interlayer of silver oxide may form because the devices are stored and tested in ambient conditions. A thin oxide layer could significantly increase the work function of the metal, to as high 5.1 eV,[25] matching it perfectly for hole collection. Furthermore, silver oxide is a semiconductor often exhibiting p-type conductivity, which may be acting as a rather efficient hole collection layer in this instance. As demonstrated in Figure 2c, the device incorporating a pure Ag electrode exhibits the highest efficiency of 4.5%. The solar cell performance parameters are shown as a table inset to Figure 2c.

There exist many external factors during the fabrication of these solar cells, which lead to a relatively large batch-to-batch variation in performance although trends within batches are consistently reproduced. In Figure 3, we present the *JV* curve measured under AM 1.5 simulated solar illumination at 126 mW cm^{-2} for our best performing solar cell, incorporating K68 sensitizer with Ag electrodes. This device exhibits a record power conversion efficiency of 5.1%, representing a new benchmark for this technology. The average efficiency for a batch of eight separate devices was $4.7 \pm 0.3\%$. We are currently pursuing alternative routes to further enhance the light capture in this solar cell, including incorporating scattering layers and macrostructuring the electrodes. Full optical modeling of the system is also being carried out in order to understand how best to enhance the light absorption.

In summary, we have synthesized a series of "ion-coordinating" ruthenium complexes for solid-state dye-sensitized solar cells and found that incorporating diblock ethylene-oxide:alkane pendent groups results in the largest suppression of charge recombination and the highest power conversion efficiency. By replacing dissipative Au electrodes with reflective Ag electrodes, we have further enhanced the light absorption in the device with a record power conversion efficiency of 5.1% having been achieved under high-intensity simulated sun light. Further leaps in efficiencies are expected by considering and improving the photonic structure of this solar cell.

Acknowledgment. H.J.S. thanks Clare College Cambridge for current funding.

References

(1) Oregan, B.; Gratzel, M. *Nature* **1991**, *353*, 737−740.
(2) Clifford, J. N.; Palomares, E.; Nazeeruddin, M. K.; Gratzel, M.; Durrant, J. R. *J. Phys. Chem. B* **2007**, *111*, 6561−6567.
(3) Ito, S.; Zakeeruddin, S. M.; Humphry-Baker, R.; Liska, P.; Charvet, R.; Comte, P.; Nazeeruddin, M. K.; Pechy, P.; Takata, M.; Miura, H.; Uchida, S.; Gratzel, M. *Adv. Matter.* **2006**, *18*, 1202.
(4) Kim, S.; Lee, J. K.; Kang, S. O.; Ko, J.; Yum, J. H.; Fantacci, S.; De Angelis, F.; Di Censo, D.; Nazeeruddin, M. K.; Gratzel, M. *J. Am. Chem. Soc* **2006**, *128*, 16701−16707.
(5) Kroeze, J. E.; Hirata, N.; Koops, S.; Nazeeruddin, M. K.; Schmidt-Mende, L.; Gratzel, M.; Durrant, J. R. *J. Am. Chem. Soc* **2006**, *128*, 16376−16383.
(6) Nazeeruddin, M. K.; Bessho, T.; Cevey, L.; Ito, S.; Klein, C.; De Angelis, F.; Fantacci, S.; Comte, P.; Liska, P.; Imai, H.; Graetzel, M. *J. Photochem. Photobiol., A* **2007**, *185*, 331−337.
(7) Bonhote, P.; Moser, J. E.; Humphry-Baker, R.; Vlachopoulos, N.; Zakeeruddin, S. M.; Walder, L.; Gratzel, M. *J. Am. Chem. Soc.* **1999**, *121*, 1324−1336.
(8) Bach, U.; Lupo, D.; Comte, P.; Moser, J. E.; Weissortel, F.; Salbeck, J.; Spreitzer, H.; Gratzel, M. *Nature* **1998**, *395*, 583−585.
(9) O'Regan, B.; Lenzmann, F.; Muis, R.; Wienke, J. *Chem. Mater.* **2002**, *14*, 5023−5029.
(10) Tennakone, K.; Kumara, G. R. R. A.; Kumarasinghe, A. R.; Wijayantha, K. G. U.; Sirimanne, P. M. *Semicond. Sci. Technol.* **1995**, *10*, 1689−1693.
(11) Poplavskyy, D.; Nelson, J. *J. Appl. Phys.* **2003**, *93*, 341−346.
(12) Kruger, J.; Plass, R.; Gratzel, M.; Cameron, P. J.; Peter, L. M. *J. Phys. Chem. B* **2003**, *107*, 7536−7539.
(13) Schmidt-Mende, L.; Gratzel, M. *Thin Solid Films* **2006**, *500*, 296−301.
(14) Snaith, H. J.; Schmidt-Mende, L.; Chiesa, M.; Gratzel, M. *Phys. Rev. B.* **2006**, *74*, 045306.
(15) Snaith, H. J.; Gratzel, M. *Appl. Phys. Lett.* **2006**, *89*, 262114.
(16) Seaman, C. H. *Solar Energy* **1982**, *29*, 291−298.
(17) O'Regan, B. C.; Durrant, J. R. *J. Phys. Chem. B* **2006**, *110*, 8544−8547.
(18) O'Regan, B. C.; Lenzmann, F. *J. Phys. Chem. B* **2004**, *108*, 4342−4350.
(19) Kruger, J.; Plass, R.; Cevey, L.; Piccirelli, M.; Gratzel, M.; Bach, U. *Appl. Phys. Lett.* **2001**, *79*, 2085−2087.
(20) Clifford, J. N.; Palomares, E.; Nazeeruddin, M. K.; Gratzel, M.; Nelson, J.; Li, X.; Long, N. J.; Durrant, J. R. *J. Am. Chem. Soc* **2004**, *126*, 5225−5233.
(21) Kuang, D.; Klein, C.; Snaith, H. J.; Humphry-Baker, R.; Moser, J.-E.; Zakeeruddin, S. M.; Grätzel, M. *Nano Lett.* **2006**, *6*, 769−773.
(22) Snaith, H. J.; Zakeeruddin, S. M.; Schmidt-Mende, L.; Klein, C.; Gratzel, M. *Angew. Chem., Int. Ed.* **2005**, *44*, 6413−6417.
(23) Kuang, D.; Klein, C.; Snaith, H. J.; Humphry-Baker, R.; Zakeeruddin, S. M.; Grätzel, M. *Inorg. Chim. Acta.* **2007**, in press, http://dx.doi.org/10.1016/j.ica.2007.05.031.
(24) Tengstedt, C.; Osikowicz, W.; Salaneck, W. R.; Parker, I. D.; Hsu, C. H.; Fahlman, M. *Appl. Phys. Lett.* **2006**, *88*, 053502.
(25) Barik, U. K.; Srinivasan, S.; Nagendra, C. L.; Subrahmanyam, A. *Thin Solid Films* **2003**, *429*, 129−134.

NL071656U